frontiers | Frontiers in Forests and Global Change

Regulation of NDVI and ET negative responses to increased atmospheric vapor pressure deficit by water availability in global drylands

Rihong Wen[1†], Peng Jiang[1,2†], Meiou Qin[3], Qingyu Jia[1],
Nan Cong[4], Xiaoying Wang[1], Ying Meng[2], Feiyun Yang[5], Bin Liu[2],
Mengyuan Zhu[6], Jiaxing Zu[7*] and Ning Chen[8*]

[1]Institute of Atmospheric Environment, China Meteorological Administration, Shenyang, China, [2]China Meteorological Administration Training Center of Liaoning, Shenyang, China, [3]Regional Climate Center of Shenyang, Shenyang, China, [4]Key Laboratory of Ecosystem Network Observation and Modeling, Institute of Geographic Sciences and Natural Resources Research, Chinese Academy of Sciences, Beijing, China, [5]China Meteorological Administration Training Center, Beijing, China, [6]College of Agronomy, Shenyang Agricultural University, Shenyang, China, [7]Ministry of Education Key Laboratory of Environment Change and Resources Use in Beibu Gulf, Nanning Normal University, Nanning, China, [8]Key Laboratory of Wetland Ecology and Environment, Northeast Institute of Geography and Agroecology, Chinese Academy of Sciences, Changchun, China

Atmospheric vapor pressure deficit (VPD, indicative of atmospheric water conditions) has been identified as a major driver of global vegetation dynamics. Drylands, including deserts, temperate grasslands, savannas, and dry forests, are more sensitive to water conditions and affect carbon, nitrogen, and water cycles. However, our knowledge is limited on the way increasing VPD affects vegetation growth and evapotranspiration (ET) in global drylands. In this study, we used long-term satellite datasets combined with multiple statistical analyses to examine the relationship between the satellite-derived normalized difference vegetation index (NDVI), a proxy for vegetation growth, and ET to VPD across global drylands. We found that significant decreases in NDVI and ET predominantly influenced the NDVI ($R_{VPD-NDVI}$) and ET (R_{VPD-ET}) responses to VPD in both the savannas and dry forests of South American, African, and Australian savannas and dry forests, as well as in temperate grasslands (e.g., Eurasian steppes and American prairies). Notably, more than 60% of global drylands exhibited significantly negative $R_{VPD-NDVI}$ and R_{VPD-ET} values. In contrast, the percentage of significantly negative $R_{VPD-NDVI}$ and R_{VPD-ET} decreased to <10% in cold drylands (>60° N). In predominantly warm drylands (60° N~60° S), negative VPD effects were significantly and positively regulated by soil water availability, as determined by multiple linear regression models. However, these significant regulatory effects were not observed in cold drylands. Moving-window analyses further revealed that temporal changes in $R_{VPD-NDVI}$ and R_{VPD-ET} were positively correlated with changes in the Standardized Precipitation Evapotranspiration Index (SPEI). In warm drylands, areas with increasing $R_{VPD-NDVI}$ and R_{VPD-ET} over time showed an increasing trend in the SPEI, whereas areas with a decreasing SPEI showed a negative trend in $R_{VPD-NDVI}$ and R_{VPD-ET} values over time. Given the increasing atmospheric dryness due to climate change, this study highlighted the importance of re-evaluating the representation of the role of water availability in driving the response of the carbon-water cycle to increased VPD across global drylands.

1. Introduction

Drylands [areas characterized by an aridity index (AI) of <0.65] cover ~41% of Earth's land surface and include deserts, temperate grasslands, savannas, and dry forests (Prăvălie, 2016; Huang et al., 2017; Lian et al., 2021). Dryland ecosystems play an important role in regulating the global carbon (Ahlstrom et al., 2015), nitrogen (Tian et al., 2020), and water (Wang et al., 2012) cycles. For example, trends and variability in the global terrestrial carbon sink are largely dominated by drylands because of drylands' sensitivity to variations in temperature and precipitation (Ahlstrom et al., 2015). A growing body of evidence shows that the ecological processes in global drylands are always driven by precipitation or soil water availability (Niu et al., 2008; Hoover et al., 2014; Chen et al., 2020a; Lian et al., 2021). Atmospheric water demand, which is characterized by a vapor pressure deficit (VPD), has been identified as a critical driver of vegetation dynamics (Yuan et al., 2019; Liu et al., 2020) and carbon balance (He et al., 2022), but it has always been overlooked in the global drylands. Recent studies have shown that dryland grasslands in the United States are even more sensitive to VPD than precipitation variations (Konings et al., 2017). Therefore, a comprehensive representation of VPD's effects in drylands would deepen our understanding of global vegetation dynamics under climate change.

Atmospheric water demand (represented by VPD) could control plant photosynthesis and transpiration by affecting the stomatal activity and xylem conductance (Rogiers et al., 2012). VPD, the difference between saturated and actual vapor pressure, is a good indicator of atmospheric water demand (Novick et al., 2016; Rigden and Salvucci, 2017). It has experienced a significant increasing trend over the past few decades and is projected to increase continually throughout the coming century (Yuan et al., 2019; Fang et al., 2022). In response to the excessive water deficit caused by a high VPD, plants tend to close their stomata and reduce the risk of hydraulic failure at the cost of reducing or stopping photosynthesis (Rogiers et al., 2012; Sulman et al., 2016). More importantly, the elevated VPD may increase the hydraulic burden on plants and subsequently limit vegetation growth, especially in regions with severe seasonal or annual water deficits (Ding et al., 2018). Despite the growing awareness and concern, only a handful of studies have been conducted to assess the impact of VPD on global drylands. This can be partly attributed to the fact that most studies focused on water balances using precipitation-based drought indices (Novick et al., 2016; Rigden and Salvucci, 2017). As a result, atmospheric water conditions, which are an essential component of the soil–plant–atmosphere continuum, have not been adequately addressed.

VPD effects could be regulated by water availability. Soil water availability is the direct water pool of plants and determines the amount of water available for plant roots (Liu et al., 2020). Soil water conditions can regulate the abscisic acid concentrations and leaf water potential, which are closely related to stomatal activities (Rogiers et al., 2012; Chen et al., 2021). For example, plant xylems or roots can respond to a soil water deficit by sensing decreased abscisic acid concentrations and closing their stomata (Rogiers et al., 2012). In addition, changes in soil water conditions could affect VPD variations by directly influencing air temperature and relative humidity, subsequently regulating VPD effects (Chen et al.,

2021). The dependence of VPD effects on soil water conditions has been investigated in studies on forests (Sulman et al., 2016), Semillon vines (Rogiers et al., 2012), and crops (Kimm et al., 2020). Compared with these relatively well-studied ecosystems, most dryland ecological processes are more sensitive to variability in water conditions (Chen et al., 2021; Lian et al., 2021). Further, it is expected that natural hazard events, particularly those of a climatic nature (especially droughts, heat waves, and wildfire activity), will become more widespread, frequent, and severe (Middleton and Sternberg, 2013). Thus, the regulatory effects of soil water content (SWC) may be important for understanding the VPD effects in global drylands.

In this study, we used long-term satellite observations of the Normalized Difference Vegetation Index (NDVI), a proxy for vegetation growth, and ET to investigate the response of ET and NDVI to VPD and soil water conditions in regulating the effects of VPD. Based on these datasets, our objectives were (1) to investigate the response of NDVI and ET to VPD in global drylands and (2) to investigate the dependence of the effects of VPD on soil water conditions. Achieving these objectives will improve our understanding of drylands' vulnerability to hydrological and climatic change and the modeling of dryland carbon and water cycle feedback to climatic change.

2. Materials and methods

2.1. Study regions

The aridity index is the ratio of mean annual precipitation to mean annual potential evapotranspiration (PET) and is used to identify cold drylands where the AI is <0.65 (Figure 1) (Middleton and Sternberg, 2013; Lian et al., 2021). The pixels with a mean annual NDVI lower than 0.1 were removed in our study to reduce noise from non-vegetated and sparsely vegetated areas. Drylands north of 60° N were defined as cold drylands, and other regions were defined as warm drylands. Warm-dryland vegetation types mainly include savannas and dry forests in South America, Africa, and Australia, as well as temperate grasslands (e.g., Eurasian steppes and American prairies) (Middleton and Sternberg, 2013; Liu et al., 2022).

2.2. Datasets

The third-generation NDVI (NDVI3g) dataset was from the Global Inventory Monitoring and Modeling Studies (GIMMS) group, derived from NOAA/AVHRR land datasets with a spatial resolution of 0.08° and a 16-day interval (Pinzon and Tucker, 2014). The GIMMS NDVI 3 g data include corrections for sensor degradation, cloud cover, inter-sensor differences, solar zenith angle, viewing angle effects, and volcanic aerosols. It has been widely used to study vegetation dynamics under climate change (Piao et al., 2014; Jiao et al., 2021). Monthly ET was derived from the Global Land Evaporation Amsterdam Model (GLEAM, v3.5a) at a spatial resolution of 0.25° (Martens et al., 2017). Potential evaporation estimates for the land fractions of bare soil, tall canopy, and short canopy were converted to actual evaporation

FIGURE 1
Spatial distribution of global drylands.
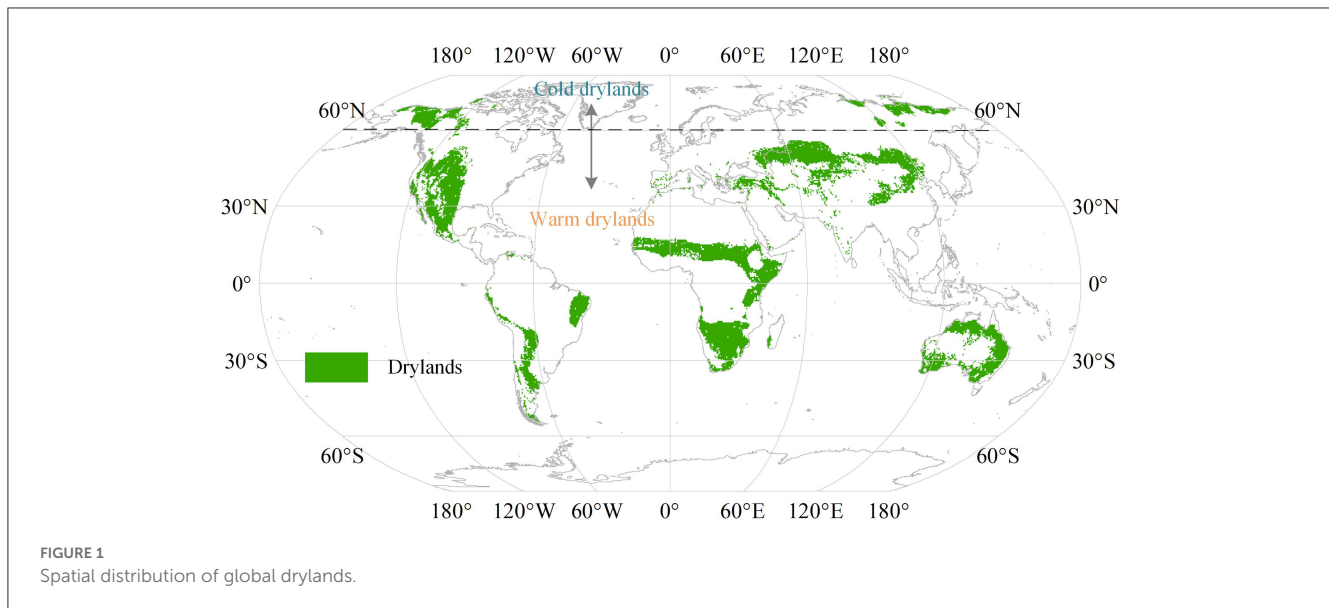
using a multiplicative evaporative stress factor based on microwave vegetation optical depth observations and root-zone soil moisture estimates (Martens et al., 2017). The aforementioned datasets were standardized to a spatial resolution of 0.5° and a 1-month temporal resolution.

Monthly solar radiation (SR) was derived from ERA-5 reanalysis products (0.1° × 0.1°) (Dee et al., 2011). Monthly root-zone SWC was derived from GLEAM v3.5a with a spatial resolution of 0.25°, which is calculated by a multi-layer running-water balance (Martens et al., 2017). Monthly air temperature (Ta), precipitation, and VPD (equations 1–2) (Yuan et al., 2019) were derived from the CRUST 4.04 dataset (land; 0.5° × 0.5°) (Harris et al., 2020). The aridity index is the ratio of mean annual precipitation to mean PET and was used to identify drylands where the AI is <0.65 (Figure 1) (Lian et al., 2021).

$$SVP = 0.611 \times \exp\left(\frac{17.27 \times Ta}{273.3 + Ta}\right) \qquad (1)$$

$$VPD = SVP - AVP \qquad (2)$$

AVP (derived from CRUST 4.04; 0.5° × 0.5°) and SVP are actual and saturated vapors, respectively. The gridded Standardized Precipitation Evapotranspiration Index (SPEI) dataset (SPEIbase v2.5) is at a 0.5° spatial resolution and monthly time step. In this study, the SPEI time scales of 1 and 3 months were used to quantify dry-wet conversions during the period of 1982–2015.

2.3. Statistical analyses

The growing season was defined as the months in which NDVI was >20% of the monthly maximum for the year in each grid cell. Partial correlation analysis (PCOR) was used to estimate the impacts of VPD on vegetation growth and ET during the growing seasons from 1982–2015 when Ta, precipitation, and SR were removed. Following previous studies (Sulman et al., 2016;

Kimm et al., 2020; Chen et al., 2021), we applied a multiple linear regression model to test the regulatory effect of SWC on VPD impacts through the interaction between VPD and SWC (VPD × SWC).
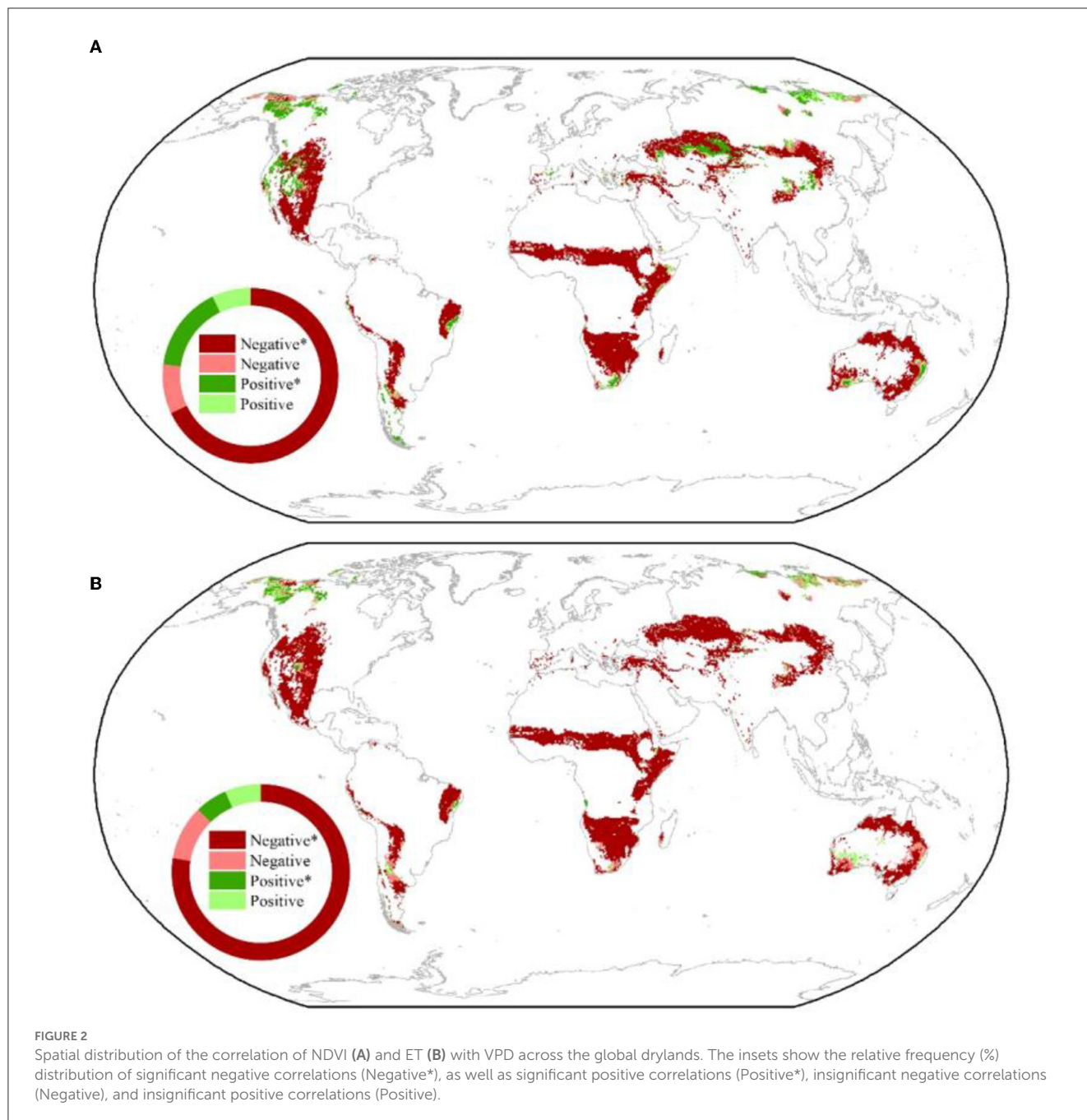
$$
\begin{aligned}
LAI \ (and \ ET) \ = \ &VPD + SWC + VPD + SWC \\
&+ \ precipitation + SR + Ta + \varepsilon \qquad (3)
\end{aligned}
$$

To further demonstrate the regulatory effect of water availability, we analyzed the temporal dynamics of VPD effects and SPEI for 1982–2015. First, we calculated the temporal variability of SPEI and the PCOR coefficients of VPD vs. LAI and ET ($R_{VPD-NDVI}$ and R_{VPD-ET}) in 25 10-year moving windows using non-parametric Mann-Kendall test (MK) analyses. We then used a simple linear regression to estimate the correlation of the temporal changes in SPEI with the temporal dynamics of $R_{VPD-NDVI}$ and R_{VPD-ET} in the 25 10-year moving windows. The aforementioned analyses were conducted in R 4.1.2 (http://www.r-project.org/).

3. Results

3.1. Responses of NDVI and ET to VPD

The significant negative response of NDVI and ET to VPD was observed mostly in global drylands. PCOR showed that NDVI and ET were significantly negatively correlated with VPD in 68.0% and 77.6% of the drylands, respectively (Figures 2A, B). These significant responses were mainly found in the warm drylands, such as savannas and dry forests in South America, Africa, and Australia, and temperate grasslands (e.g., Eurasian steppes and American prairies) (Figures 2A, B). In contrast, significant positive responses of NDVI and ET to VPD were detected throughout 53.3% and 36.4% of the cold drylands, respectively, whereas the percentage decreased to 4.1% and 6.8% for the significant negative responses (Figures 2A, B). These results suggested that the suppression of

FIGURE 2
Spatial distribution of the correlation of NDVI **(A)** and ET **(B)** with VPD across the global drylands. The insets show the relative frequency (%) distribution of significant negative correlations (Negative*), as well as significant positive correlations (Positive*), insignificant negative correlations (Negative), and insignificant positive correlations (Positive).

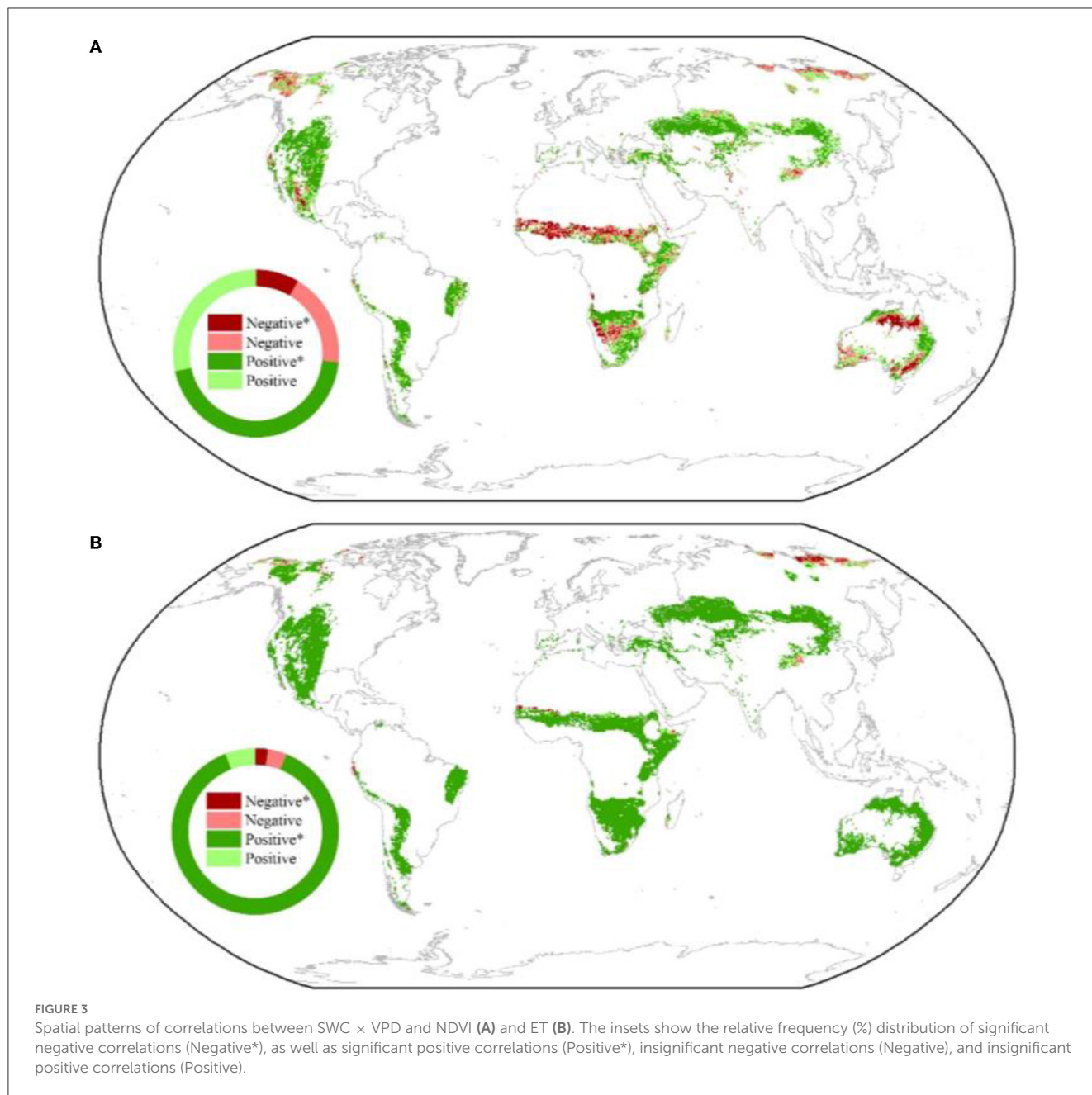NDVI and ET by VPD was stronger in warm drylands than in cold drylands.

3.2. SWC regulated the VPD effects

The responses of NDVI and ET to VPD were significantly regulated by soil water availability in global drylands. A significant positive correlation in the interaction of VPD×SWC with NDVI and ET was observed in 44.9% and 88.1% of the drylands, respectively, but the VPD×SWC was significantly and negatively correlated with NDVI and ET in only 8.4% and 2.5% of the drylands, respectively (Figures 3A, B). The percentages of the

significant positive effects of VPD × SWC on NDVI and ET were ∼40% lower in the cold drylands than in the warm drylands (Figures 3A, B). Overall, these results suggest that the suppression of NDVI and ET by VPD could be mitigated in the global drylands by improving the water supply.

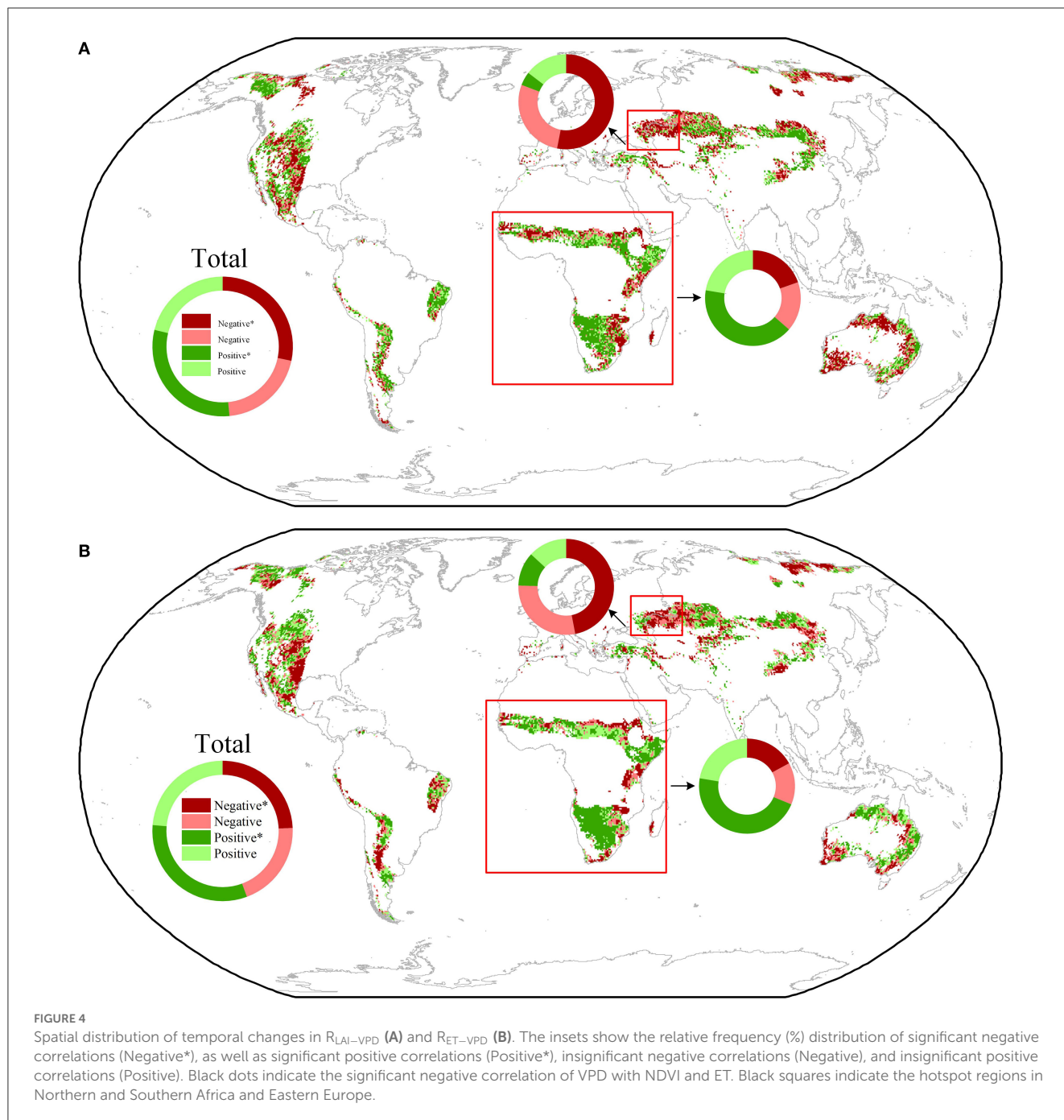## 3.3. Temporal changes in VPD effects with changes in water supply

We analyzed the temporal dynamics in the response of NDVI and ET to VPD to investigate the regulatory effects of water availability on the effects of VPD. The moving-window analyses

FIGURE 3
Spatial patterns of correlations between SWC × VPD and NDVI **(A)** and ET **(B)**. The insets show the relative frequency (%) distribution of significant negative correlations (Negative*), as well as significant positive correlations (Positive*), insignificant negative correlations (Negative), and insignificant positive correlations (Positive).

showed that significant increases in $R_{VPD-NDVI}$ and R_{VPD-ET} were found in 30.4 % and 32.0 % of the drylands, respectively, and $R_{VPD-NDVI}$ and R_{VPD-ET} showed significant decreasing trends in 28.3% and 24.3% of the study regions, respectively (Figures 4A, B). Significant temporal changes in $R_{VPD-NDVI}$ and R_{VPD-ET} were observed in the warm drylands of Northern and Southern Africa and Eastern Europe in dense concentrations (Figures 4A, B). In Northern and Southern Africa, $R_{VPD-NDVI}$ and R_{VPD-ET} experienced significant increases in 41.2% and 46.3% of the dryland regions, respectively; in Eastern Europe, significant decreases in $R_{VPD-NDVI}$ and R_{VPD-ET} were observed in 53.0% and 47.5% of the dryland regions, respectively (Figures 4A, B).

To further investigate whether the observed temporal changes in $R_{VPD-NDVI}$ and R_{VPD-ET} were caused by changes in water supply, we analyzed the correlation of the temporal dynamics of water supply with temporal changes in VPD effects in the 25 10-year moving windows. Our observations showed that the areas where SPEI decreased (increased) often corresponded to the areas where $R_{VPD-NDVI}$ and R_{VPD-ET} decreased (increased) (Figures 5A, B). Increases (significant, 38.3 %; insignificant, 34.8%) in SPEI dominated the temporal changes in water availability in the warm drylands of northern and southern Africa (Figures 5A, B). In contrast, the temporal changes in water availability in Eastern Europe were dominated by decreases in SPEI (significant, 5.1%; insignificant, 71.0 %) (Figures 5A, B). We further found that temporal changes in SWC were significantly positively correlated with changes in $R_{VPD-NDVI}$ (R_{VPD-ET}) in 62.5 % (65.3%) of Eastern Europe and in 33.9 % (40.0%) of Africa (Figures 5C, D).

FIGURE 4
Spatial distribution of temporal changes in $R_{LAI-VPD}$ **(A)** and R_{ET-VPD} **(B)**. The insets show the relative frequency (%) distribution of significant negative correlations (Negative*), as well as significant positive correlations (Positive*), insignificant negative correlations (Negative), and insignificant positive correlations (Positive). Black dots indicate the significant negative correlation of VPD with NDVI and ET. Black squares indicate the hotspot regions in Northern and Southern Africa and Eastern Europe.
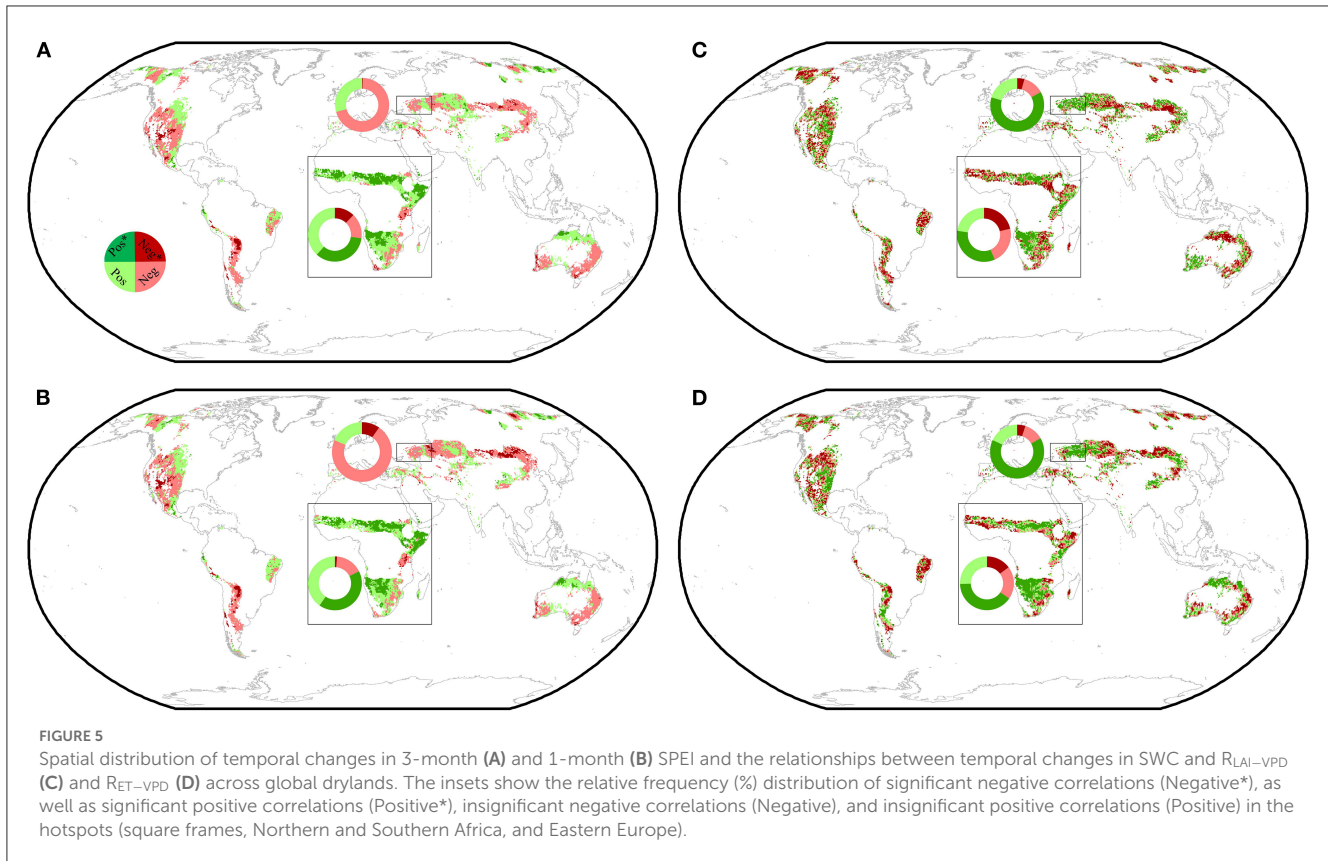
Taken together, these observations emphasized that improving water availability alleviated VPD's suppression of NDVI and ET in Africa, and with increasing water deficits, the VPD's suppressing effect was magnified.

4. Discussion

The VPD-induced suppressions are consistent with the results of previous studies in the temperate grasslands of the dryland regions (Niu et al., 2008; Konings et al., 2017; Ding et al., 2018; Chen et al., 2020a). These grassland regions are characterized by

limited precipitation of 300–500 mm, poor water-holding capacity associated with stony sandy loam, and stronger solar radiation and wind (Chen et al., 2021; Lian et al., 2021). Grasses, as particularly abundant species in global drylands, have relatively shallow root systems (Liu et al., 2022), which are limited by dry surface soils (Zhang et al., 2018; Chen et al., 2020b). This could be further exacerbated because dry soils restrict root growth (Niu et al., 2008), making the remaining soil moisture less accessible for uptake as the soil suction increases (Seneviratne et al., 2010). In the areas where these occur, the tendency may be for leaves to limit their stomatal activity with a water-conservative strategy in response to increasing VPD (Massmann et al., 2019). As a result, photosynthesis is

FIGURE 5
Spatial distribution of temporal changes in 3-month (A) and 1-month (B) SPEI and the relationships between temporal changes in SWC and $R_{LAI-VPD}$ (C) and R_{ET-VPD} (D) across global drylands. The insets show the relative frequency (%) distribution of significant negative correlations (Negative*), as well as significant positive correlations (Positive*), insignificant negative correlations (Negative), and insignificant positive correlations (Positive) in the hotspots (square frames, Northern and Southern Africa, and Eastern Europe).

reduced, and water loss is limited to reduce the risk of hydraulic failure (Meinzer et al., 2016).

NDVI and ET were also significantly suppressed by VPD in the seasonally dry dryland savannas of South America, Africa, and Australia. Although savanna woodlands may use deep soil water through their vigorous root systems to maintain stomatal openness, plants can suppress stomatal activity and vegetation growth as the water deficit strengthens during the dry seasons. These observations have been supported by a recent study conducted in seasonal dry subtropical forests (Chen et al., 2021). This could be attributable to Xeric species adopting a more conservative sequence to prevent severe tissue damage through tighter stomatal regulation (isohydric strategy) and higher embolism resistance (Jin et al., 2023), especially for the sunnier and drier seasons (Konings and Gentine, 2017).

Ecological processes in drylands may be broadly more resilient to changes in water availability (Hoover et al., 2015). Our findings showed that water availability positively regulated the suppression of VPD on vegetation growth and ET. In the warm drylands of Africa, increases in precipitation in southern Africa and the Sahel have been demonstrated by observational and modeling evidence (Maidment et al., 2015), as well as our findings. When water availability improves more significantly, the negative sensitivity of vegetation growth and ET to VPD could be attenuated (Sulman et al., 2016; Rigden et al., 2020) and even change from significantly negative to positive (Chen et al., 2021). This could be due to the following reasons: First, the rapid recovery of soil water has direct effects on soil evaporation, thereby mitigating atmospheric dryness,

which could otherwise be more severe by further aggravating water stress (Chen et al., 2021); second, when the soil water supply is improved, which is often associated with increasing leaf water potential and decreasing abscisic acid, photosynthesis is improved by the maintenance of transpiration and evaporative cooling (Rogiers et al., 2012).

In contrast, climate scenarios and our observations showed increased water deficits and heatwaves over the past few decades in Eastern Europe (Seneviratne et al., 2010; Liu et al., 2021). In particular, frequent heatwaves associated with high temperatures and low SWC exacerbate the negative impacts of VPD on vegetation growth and ET by pushing atmospheric dryness to its peak (Wang et al., 2020; Fu et al., 2022). Thus, VPD-induced suppression is exacerbated on a temporal scale by declining water supplies in Eastern Europe.

In addition to water availability, increasing atmospheric CO_2 is an important factor regulating VPD effects in global drylands. Recent studies have shown that the negative effects of VPD on dryland vegetation growth may be partially offset by increasing CO_2 (Ding et al., 2018). This is not surprising as atmospheric CO_2 regulates stomatal conductance, which is directly related to plant photosynthesis (de Boer et al., 2011). Furthermore, CO_2-induced water savings are sufficient to alleviate water limitation and allow for continued photosynthesis in drylands (Morgan et al., 2011; Lian et al., 2021). We found that, when CO_2 was included in the PCOR models, $R_{VPD-NDVI}$ and R_{VPD-ET} were increased by 0.01 and 0.09, respectively, in over 50% of the global drylands compared to CO_2 removal (unpublished data), which is consistent with these studies.

This signifies that the positive water-saving effects of CO_2 could neutralize the suppression of VPD on the carbon-water cycle.

Compared to the warm drylands, a weaker VPD suppression was found in the cold drylands. Most cold drylands are distributed in the tundra biome. More available soil moisture in the tundra under favorable atmospheric conditions would maintain air humidity, as evidenced by slight increases in RH (Vicente-Serrano et al., 2018). Furthermore, in cold ecosystems, climate warming may improve vegetation growth by enhancing soil organic matter decomposition and nitrogen mineralization (Rustad et al., 2001; Lu et al., 2013; Wang et al., 2019). Increased below-ground biomass could potentially be beneficial for extracting more water from moisture-rich soils (Li et al., 2020). With increases in VPD, adequate moisture can not only maintain high leaf water potential but also potentially respond to atmospheric water demand, which could alleviate VPD-induced suppression.

Our study has several limitations. Although a recent study reported that dryland grasses with a water-conserving strategy responded to increased VPD at the site scale (Massmann et al., 2019), the plant water-use strategy was not measured at the large spatial scale of drylands. Furthermore, many indicators (e.g., leaf hydraulic traits) related to plant water-use strategy were not measured in this study. These indicators may also shape the ecological response mechanisms of vegetation growth and ET to VPD, especially during dry-wet transitions (Rogiers et al., 2012; Novick et al., 2019). Given the above, future field experiments should comprehensively measure these indicators to better understand VPD effects throughout global drylands.

5. Conclusions

Dryland ecosystems play a critical role in the global carbon, nitrogen, and water cycles and are among the most vulnerable ecosystems to climate change. Using long-term satellite datasets, we found that increases in VPD in global drylands had a wide range of ecological consequences, ranging from the suppression of vegetation growth to the reduction of ET. This VPD-induced suppression of vegetation growth and ET was significantly and positively regulated by changes in water availability across the global drylands. Based on our analyses, future VPD-induced suppression in global drylands could be relieved as soil water increases in the coming century (Lian et al., 2021). For the global drylands, this study deepened our understanding of the response of carbon and water cycles to increasing atmospheric dryness and provides more realistic projections of carbon and water cycles under climate change.

Publisher's note

All claims expressed in this article are solely those of the authors and do not necessarily represent those of their affiliated organizations, or those of the publisher, the editors and the reviewers. Any product that may be evaluated in this article, or claim that may be made by its manufacturer, is not guaranteed or endorsed by the publisher.

References

Ahlstrom, A., Raupach, M.R., Schurgers, G., Smith, B., Arneth, A., Jung, M., et al. (2015). The dominant role of semi-arid ecosystems in the trend and variability of the land CO2 sink. *Science* 348, 895–899. doi: 10.1126/science.aaa1668

Chen, N., Song, C., Xu, X., Wang, X., Cong, N., Jiang, P., et al. (2021). Divergent impacts of atmospheric water demand on gross primary productivity in three typical ecosystems in China. *Agricult. Forest Meteorol.* 307, 108527. doi: 10.1016/j.agrformet.2021.108527

Chen, N., Zhang, Y., Zhu, J., Cong, N., Zhao, G., Zu, J., et al. (2020a). Multiple-scale negative impacts of warming on ecosystem carbon use efficiency across the Tibetan Plateau grasslands. *Global Ecol. Biogeograp.* 30, 398–413. doi: 10.1111/geb.13224

Chen, N., Zhang, Y., Zu, J., Zhu, J., Zhang, T., Huang, K., et al. (2020b). The compensation effects of post-drought regrowth on earlier drought loss across the tibetan plateau grasslands. *Agricult. Forest Meteorol.* 281, 107822. doi: 10.1016/j.agrformet.2019.107822

de Boer, H.J., Lammertsma, E.I., Wagner-Cremer, F., Dilcher, D.L., Wassen, M.J., and Dekker, S.C. (2011). Climate forcing due to optimization of maximal leaf conductance in subtropical vegetation under rising CO2. *Proceed. Nat. Acad. Sci.* 108, 4041–4046. doi: 10.1073/pnas.1100555108

Dee, D.P., Uppala, S.M., Simmons, A., Berrisford, P., Poli, P., Kobayashi, S., et al. (2011). The ERA-Interim reanalysis: configuration and performance of the data assimilation system. *Q. J. R. Meteorol. Soc.* 137, 553–597. doi: 10.1002/qj.828

Ding, J., Yang, T., Zhao, Y., Liu, D., Wang, X., Yao, Y., et al. (2018). Increasingly important role of atmospheric aridity on Tibetan alpine grasslands. *Geophys. Res. Lett.* 45, 2852–2859. doi: 10.1002/2017GL076803

Fang, Z., Zhang, W., Brandt, M., Abdi, A.M., and Fensholt, R. (2022). Globally increasing atmospheric aridity over the 21st century. *Earth's Future* 10, e2022EF003019. doi: 10.1029/2022ef003019

Fu, Z., Ciais, P., Prentice, I.C., Gentine, P., Makowski, D., Bastos, A., et al. (2022). Atmospheric dryness reduces photosynthesis along a large range of soil water deficits. *Nat. Commun.* 13, 989. doi: 10.1038/s41467-022-28652-7

Harris, I., Osborn, T. J., Jones, P., and Lister, D. (2020). Version 4 of the CRU TS monthly high-resolution gridded multivariate climate dataset. *Scientific Data.* 7:109. doi: 10.1038/s41597-020-0453-3

He, B., Chen, C., Lin, S., Yuan, W., Chen, H.W., Chen, D., et al. (2022). Worldwide impacts of atmospheric vapor pressure deficit on the interannual variability of terrestrial carbon sinks. *Nat. Sci. Rev.* 9, nwab150. doi: 10.1093/nsr/nwab150

Hoover, D.L., Duniway, M.C., and Belnap, J. (2015). Pulse-drought atop press-drought: unexpected plant responses and implications for dryland ecosystems. *Oecologia* 179, 1211–1221. doi: 10.1007/s00442-015-3414-3

Hoover, D.L., Knapp, A.K., and Smith, M.D. (2014). Resistance and resilience of a grassland ecosystem to climate extremes. *Ecology* 95, 2646–2656.

Huang, J., Li, Y., Fu, C., Chen, F., Fu, Q., Dai, A., et al. (2017). Dryland climate change: Recent progress and challenges. 55, 719–778.

Jiao, W., Wang, L., Smith, W.K., Chang, Q., Wang, H., and D'Odorico, P. (2021). Observed increasing water constraint on vegetation growth over the last three decades. *Nat. Commun.* 12, 3777. doi: 10.1038/s41467-021-24016-9

Jin, Y., Hao, G., Hammond, W.M., Yu, K., Liu, X., Ye, Q., et al. (2023). Aridity-dependent sequence of water potentials for stomatal closure and hydraulic dysfunctions in woody plants. *Global Change Biol.* 3, 605. doi: 10.1111/gcb.16605

Kimm, H., Guan, K., Gentine, P., Wu, J., Bernacchi, C.J., Sulman, B.N., et al. (2020). Redefining droughts for the U.S. Corn Belt: the dominant role of atmospheric vapor pressure deficit over soil moisture in regulating stomatal behavior of Maize and Soybean. *Agricult. Forest Meteorol.* 287, 107930. doi: 10.1016/j.agrformet.2020.107930

Konings, A.G., and Gentine, P. (2017). Global variations in ecosystem-scale isohydricity. *Glob. Chang. Biol.* 23, 891–905. doi: 10.1111/gcb.13389

Konings, A.G., Williams, A.P., and Gentine, P. (2017). Sensitivity of grassland productivity to aridity controlled by stomatal and xylem regulation. *Nat. Geosci.* 10, 284–288. doi: 10.1038/ngeo2903

Li, P., Sayer, E.J., Jia, Z., Liu, W., Wu, Y., Yang, S., et al. (2020). Deepened winter snow cover enhances net ecosystem exchange and stabilizes plant community composition and productivity in a temperate grassland. *Glob. Chang. Biol.* 26, 3015–3027. doi: 10.1111/gcb.15051

Lian, X., Piao, S., Chen, A., Huntingford, C., Fu, B., Li, L. Z. X., et al. (2021). Multifaceted characteristics of dryland aridity changes in a warming world. *Nat. Rev. Earth Environ.* 2, 232–250. doi: 10.1038/s43017-021-00144-0

Liu, L., Gudmundsson, L., Hauser, M., Qin, D., Li, S., and Seneviratne, S.I. (2020). Soil moisture dominates dryness stress on ecosystem production globally. *Nat. Commun.* 11, 4892. doi: 10.1038/s41467-020-18631-1

Liu, L., Sayer, E.J., Deng, M., Li, P., Liu, W., Wang, X., et al. (2022). The grassland carbon cycle: Mechanisms, responses to global changes, and potential contribution to carbon neutrality. *Fundam. Res.* 4, 28. doi: 10.1016/j.fmre.2022.09.028

Liu, X., He, B., Guo, L., Huang, L., Yuan, W., Chen, X., et al. (2021). European carbon uptake has not benefited from vegetation greening. *Geophys. Res. Lett.* 48, 4870. doi: 10.1029/2021gl094870

Lu, M., Zhou, X., Yang, Q., Li, H., Luo, Y., Fang, C., et al. (2013). Responses of ecosystem carbon cycle to experimental warming: a meta-analysis. *Ecology* 94, 726–738. doi: 10.1890/12-0279.1

Maidment, R.I., Allan, R.P., and Black, E. (2015). Recent observed and simulated changes in precipitation over Africa. *Geophys. Res. Lett.* 42, 8155–8164. doi: 10.1002/2015gl065765

Martens, B., Miralles, D.G., Lievens, H., van der Schalie, R., de Jeu, R.A.M., Fernández-Prieto, D., et al. (2017). GLEAM v3: satellite-based land evaporation and root-zone soil moisture. *Geoscien. Model Develop.* 10, 1903–1925. doi: 10.5194/gmd-10-1903-2017

Massmann, A., Gentine, P., and Lin, C. (2019). When does vapor pressure deficit drive or reduce evapotranspiration? *J. Adv. Model. Earth Sys.* 11, 3305–3320. doi: 10.1029/2019MS001790

Meinzer, F.C., Woodruff, D.R., Marias, D.E., Smith, D.D., McCulloh, K.A., Howard, A.R., et al. (2016). Mapping 'hydroscapes' along the iso- to anisohydric continuum of stomatal regulation of plant water status. *Ecol. Lett.* 19, 1343–1352. doi: 10.1111/ele.12670

Middleton, N.J., and Sternberg, T. (2013). Climate hazards in drylands: a review. *Earth-Sci. Rev.* 126, 48–57.

Morgan, J.A., LeCain, D.R., Pendall, E., Blumenthal, D.M., Kimball, B.A., Carrillo, Y., et al. (2011). C4 grasses prosper as carbon dioxide eliminates desiccation in warmed semi-arid grassland. *Nature* 476, 202–205. doi: 10.1038/nature 10274

Niu, S., Wu, M., Han, Y., Xia, J., Li, L., and Wan, S. (2008). Water-mediated responses of ecosystem carbon fluxes to climatic change in a temperate steppe. *New Phytol.* 177, 209–219. doi: 10.1111/j.1469-8137.2007.02237.x

Novick, K.A., Ficklin, D.L., Stoy, P.C., Williams, C.A., Bohrer, G., Oishi, A.C., et al. (2016). The increasing importance of atmospheric demand for ecosystem water and carbon fluxes. *Nat. Clim. Chang.* 6, 1023–1027. doi: 10.1038/nclimate 3114

Novick, K.A., Konings, A.G., and Gentine, P. (2019). Beyond soil water potential: an expanded view on isohydricity including land-atmosphere interactions and phenology. *Plant Cell Environ.* 42, 1802–1815. doi: 10.1111/pce.13517

Piao, S., Nan, H., Huntingford, C., Ciais, P., Friedlingstein, P., Sitch, S., et al. (2014). Evidence for a weakening relationship between interannual temperature variability and northern vegetation activity. *Nat. Commun.* 5, 5018. doi: 10.1038/ncomms 6018

Pinzon, J.E., and Tucker, C.J. (2014). A non-stationary 1981–2012 AVHRR NDVI3g time series. *Remote Sens.* 6, 6929–6960. doi: 10.3390/rs6086929

Prăvălie, R. (2016). Drylands extent and environmental issues. A global approach. *Earth-Sci. Rev.* 161, 259–278. doi: 10.1016/j.earscirev.2016.08.003

Rigden, A.J., Mueller, N.D., Holbrook, N.M., Pillai, N., and Huybers, P. (2020). Combined influence of soil moisture and atmospheric evaporative demand is important for accurately predicting US maize yields. *Nature Food* 1, 127–133. doi: 10.1038/s43016-020-0028-7

Rigden, A.J., and Salvucci, G.D. (2017). Stomatal response to humidity and CO2 implicated in recent decline in US evaporation. *Glob. Chang. Biol.* 23, 1140–1151. doi: 10.1111/gcb.13439

Rogiers, S.Y., Greer, D.H., Hatfield, J.M., Hutton, R.J., Clarke, S.J., Hutchinson, P.A., et al. (2012). Stomatal response of an anisohydric grapevine cultivar to evaporative demand, available soil moisture and abscisic acid. *Tree Physiol.* 32, 249–261. doi: 10.1093/treephys/tpr131

Rustad, L., Campbell, J., Marion, G., Norby, R., Mitchell, M., Hartley, A., et al. (2001). A meta-analysis of the response of soil respiration, net nitrogen mineralization, and aboveground plant growth to experimental ecosystem warming. *Oecologia* 126, 543–562. doi: 10.1007/s004420000544

Seneviratne, S.I., Corti, T., Davin, E.L., Hirschi, M., Jaeger, E.B., Lehner, I., et al. (2010). Investigating soil moisture–climate interactions in a changing climate: a review. *Earth-Sci. Rev.* 99, 125–161. doi: 10.1016/j.earscirev.2010.02.004

Sulman, B.N., Roman, D.T., Yi, K., Wang, L., Phillips, R.P., and Novick, K.A. (2016). High atmospheric demand for water can limit forest carbon uptake and transpiration as severely as dry soil. *Geophys. Res. Lett.* 43, 9686–9695. doi: 10.1002/2016gl0 69416

Tian, H., Xu, R., Canadell, J.G., Thompson, R.L., Winiwarter, W., Suntharalingam, P., et al. (2020). A comprehensive quantification of global nitrous oxide sources and sinks. 586, 248–256.

Vicente-Serrano, S.M., Nieto, R., Gimeno, L., Azorin-Molina, C., Drumond, A., El Kenawy, A., et al. (2018). Recent changes of relative humidity: regional connections with land and ocean processes. *Earth Sys. Dynam.* 9, 915–937. doi: 10.5194/esd-9-915-2018

Wang, L., d'Odorico, P., Evans, J., Eldridge, D., McCabe, M., Caylor, K., et al. (2012). Dryland ecohydrology and climate change: critical issues and technical advances. 16, 2585–2603.

Wang, N., Quesada, B., Xia, L., Butterbach-Bahl, K., Goodale, C.L., and Kiese, R. (2019). Effects of climate warming on carbon fluxes in grasslands- A global meta-analysis. *Glob. Chang. Biol.* 25, 1839–1851. doi: 10.1111/gcb.14603

Wang, S., Zhang, Y., Ju, W., Porcar-Castell, A., Ye, S., Zhang, Z., et al. (2020). Warmer spring alleviated the impacts of 2018 European summer heatwave and drought on vegetation photosynthesis. *Agricult. Forest Meteorol.* 295, 108195. doi: 10.1016/j.agrformet.2020.108195

Yuan, W., Zheng, Y., Piao, S., Ciais, P., Lombardozzi, D., Wang, Y., et al. (2019). Increased atmospheric vapor pressure deficit reduces global vegetation growth. *Sci. Adv.* 5, eaax1396. doi: 10.1126/sciadv.aax1396

Zhang, T., Zhang, Y., Xu, M., Zhu, J., Chen, N., Jiang, Y., et al. (2018). Water availability is more important than temperature in driving the carbon fluxes of an alpine meadow on the Tibetan Plateau. *Agricult. Forest Meteorol.* 256, 22–31. doi: 10.1016/j.agrformet.2018.02.027